

Phase Relationships of Crystalline Polymorphs of Mesogenic 4-Cyano-4′-heptyloxybiphenyl (7OCB) and 4-Cyano-4′-octyloxybiphenyl (8OCB)

Kayako Hori,* Yuko Iwai, Megumi Yano,[1] Reiko Orihara-Furukawa, Yasunori Tominaga,[1] Eiji Nishibori,[2] Masaki Takata,[3] Makoto Sakata,[2] and Kenichi Kato[3]

Department of Chemistry, Ochanomizu University, Otsuka, Bunkyo-ku, Tokyo 112-8610

[1]Graduate School of Humanities and Sciences, Ochanomizu University, Otsuka, Bunkyo-ku, Tokyo 112-8610

[2]Department of Applied Physics, Nagoya University, Chikusa-ku, Nagoya 464-8603

[3]Japan Synchrotron Radiation Research Institute and CREST, Japan Science and Technology Corporation (JST), Kouto, Mikazuki-cho, Sayo-gun, Hyogo 678-5198

Received December 3, 2004; E-mail: khori@cc.ocha.ac.jp

Temperature-dependent X-ray diffraction (XRD) studies using synchrotron radiation and Raman spectral studies in the range of 40–850 cm^{-1} have been carried out for crystalline polymorphs of the title compounds in order to elucidate the phase relations of the polymorphs. Transition processes between metastable phases have been confirmed with structural evidence: square-plate (**SP**) crystal to needle (**N**) crystal for 7OCB and parallelpiped plate (**PP**) crystal to needle (**N**) crystal for 8OCB; these processes were previously proposed based on the results of differential scanning calorimetry. XRD study shows that a fourth phase of 7OCB, which appears during the stabilization process and hence is referred to as an intermediate phase, is a slightly but definitely different crystalline phase from the most stable phase. **SP** of 7OCB stabilizes in two steps: first to the intermediate phase, which then rearranges to the most stable phase at the melting point of the intermediate phase just below the melting point of the most stable phase or on keeping at RT for several months or longer. Some structural features of the most stable phases of 7OCB and 8OCB are discussed based on the unit cell parameters derived from the powder XRD results.

Reports of crystalline polymorphism are becoming common with the accumulation of crystal structural data and the phenomenon attracts a lot of attention.[1] Since the polymorphism appears depending on a subtle balance of intermolecular interactions, it is important to know the thermodynamic relationships between crystalline polymorphs in order to understand the intermolecular interactions controlling the structure-property correlations. The polymorphism is a serious issue to be handled in industries such as pharmaceuticals,[2] dyes, and pigments.[3] The recognition of the polymorphism, however, remains still accidental and the full description of the polymorphs of a compound is not always available.

4-Cyano-4′-heptyloxybiphenyl (abbr. 7OCB) and 4-cyano-4′-octyloxybiphenyl (abbr. 8OCB) have been widely studied,[4] because they are typical mesogens that form the nematic and smectic A phases, respectively, with relatively simple molecular constitutions. As for the crystalline polymorphism, it was reported that different solid phases appear from the melts, depending on the cooling rates.[5,6] Later, in the course of systematic crystal structure determination in order to obtain information on intermolecular interactions, it was found that each mesogen has four different solid phases.[7,8] 7OCB has needle (**N**) and square-plate (**SP**) crystal forms, which are metastable, while the most stable phase is found in a commercially available powder specimen (**CP**), which is produced by keeping the material at RT for long time irrespective of the original form. All the attempts to obtain single crystals of the most stable phase from solutions or from the melt have been unsuccessful. The fourth solid phase is found in a "collapsed" sample derived from **SP** by keeping it at RT for a few days. Differential scanning calorimetry (DSC) of the collapsed sample gave two successive peaks around 324–327 K, as shown in Fig. 1 (upper). Metastable **N** and **SP** also gave double peaks in the same temperature range. The higher-temperature peak corresponds to the melting of the most stable phase. We denote the fourth phase, the one responsible for the lower peak of the double peaks, as an "intermediate" phase because the phase appears on the way to stabilization of the metastable phases. The transition enthalpy estimated for each peak of the metastable crystals was highly dependent on the heating rates (0.1–10 $K\,min^{-1}$). The phase relations were proposed based on the DSC results, as shown in Fig. 1 (lower).[7] **SP** has two processes: one process is a transformation to **N** at the first endothermic DSC peak at about 314 K and the other is stabilization around RT and above to the intermediate phase and/or the most stable phase. IR spectral studies confirmed the phase change of **SP**: CN stretching bands showed changes at 299, 309–315, and 324–328 K, at the heating rate of 0.2 $K\,min^{-1}$.[9] However, the phases in the respective temperature regions could not be identified in relation to the structures, because CN bands overlapped into complicated profiles. Thus, it is an open question if **SP** stabilizes to the intermediate and the most stable phases in parallel or stepwise. In addition, no structural information has been obtained for the most stable phase or for the intermediate phase.

Published on the web July 1, 2005; DOI 10.1246/bcsj.78.1223

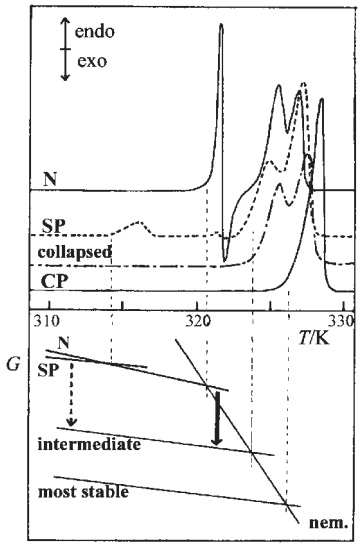

Fig. 1. DSC traces of **N**, **SP**, a collapsed sample obtained by keeping **SP** at RT, and **CP** of 7OCB at a scan rate of 1 K min^{-1} (upper) and the Gibbs energy and temperature diagram (lower). ·····→ and ——→ denote the slow and rapid stabilization processes, respectively. Rewritten from Ref. 7.

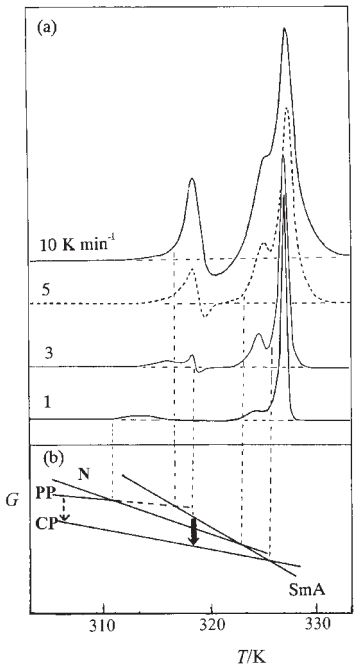

Fig. 2. DSC traces of **PP** of 8OCB at the heating rates of 1, 3, 5, and 10 K min^{-1} (upper) and the Gibbs energy and temperature diagram (lower). ·····→ and ——→ denote the slow and rapid stabilization processes, respectively. Rewritten from Ref. 8.

On the other hand, 8OCB has needle (**N**), square-plate (**SP**), parallelpiped plate (**PP**) crystal forms, which are metastable. The most stable phase is found in a commercially available powder specimen (**CP**), produced by keeping the sample at RT for long time. For 8OCB also, single crystals of the most stable phase have not been obtained. The results of DSC suggest the relations among phases as shown in Fig. 2.[8] **PP** gradually stabilizes around RT and above. In addition, **PP** transforms to **N** at about 311 K in the case of slow heating (1 K min^{-1}), while **PP** passes the transition and reaches its own melting point at 317 K in the case of rapid heating (10 K min^{-1}).

In this work, powder X-ray diffraction (XRD) studies have been carried out using a low divergent and highly brilliant beam of synchrotron radiation in order to elucidate the proposed phase relations of 7OCB more clearly and to obtain structural information on the most stable phase and the intermediate phase of 7OCB and on the most stable phase of 8OCB. Raman spectroscopy has been employed in order to compliment the conclusions for 7OCB and to elucidate the relationships for 8OCB, for which more rapid change was observed than for 7OCB: as mentioned above, the relevant heating rates were 1–10 K min^{-1}. We focused our attention on the lower wavenumber region (40–850 cm^{-1}). Spectra in this region supply information on the lattice vibrations and on the vibrations of molecular frameworks, such as C–C–C skeletal modes, which are expected to reflect the difference of crystal structures.

Experimental

Single crystals of **SP** and **N** of 7OCB and **PP** and **N** of 8OCB were obtained as previously described.[7,9]

XRD patterns were measured on a Debye–Scherrer camera[10] installed at SPring-8 BL02B2 using synchrotron radiation ($\lambda = 1.000$ Å) with a high-temperature N_2 gas flow system. Temperature was controlled at a constant value during X-ray exposure for 5 minutes and raised immediately between exposures. The heating rate on average was about 0.5 K min^{-1}. Single crystals were freshly cut into pieces with a razor and enclosed in a 0.5 mmϕ glass capillary as quickly as possible to avoid possible phase changes induced by the mechanical stresses. Thus, the intensities of XRD were influenced seriously by the effects of orientations of the crystallites.

Unit cell parameters were determined for the XRD patterns of the most stable crystalline phases of 7OCB and 8OCB by using the DASH[11] program package.

Raman spectra were measured on a JOBIN YVON T64000 Laser-Raman spectrophotometer equipped with a Mettler FP80 hot stage. Back-scattered light was detected without a polarizer. Light source, Ar^+ laser ($\lambda = 514.5$ nm); slit, 200 μm; accumulation time, 2 s; number of accumulations, 10; detection, liq. N_2 cooled CCD: sample area, ca. 10 μmϕ. Temperature dependence of the spectra was measured at the heating rate of 2 K min^{-1}. Vibrational frequencies were corrected for the line (2179.854 cm^{-1}) of a conventional fluorescent light. Resultant errors were estimated to be within ±0.7 cm^{-1} for most peaks.

Results and Discussion

XRD of 7OCB. Figure 3 shows XRD patterns for the crystalline polymorphs of 7OCB at RT. For **SP**, the *d*-values of 34.3 and 17.6 Å are (200) and (400) reflections. The very small peaks between them are components of a new phase, as shown in Fig. 4, which appeared in spite of the quick treatment mentioned in the Experimental section.

Figure 4 shows the temperature dependence of XRD of **SP**. At 313 K, the peaks of **SP** (designated by #) show a reduced

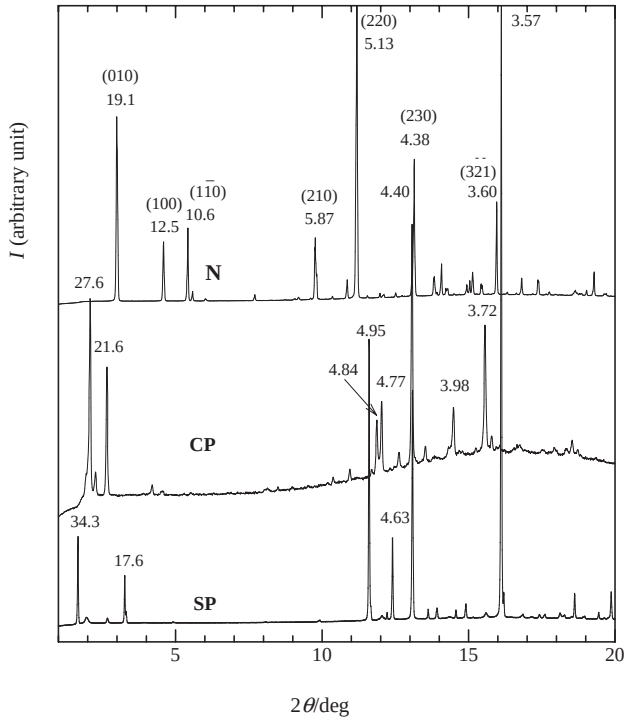

Fig. 3. XRD patterns of **N**, **CP**, and **SP** of 7OCB. Numerical values are *d*-values in Å. For **N**, *hkl*'s indexed by PULVERIX[12] are shown above the *d*-values.

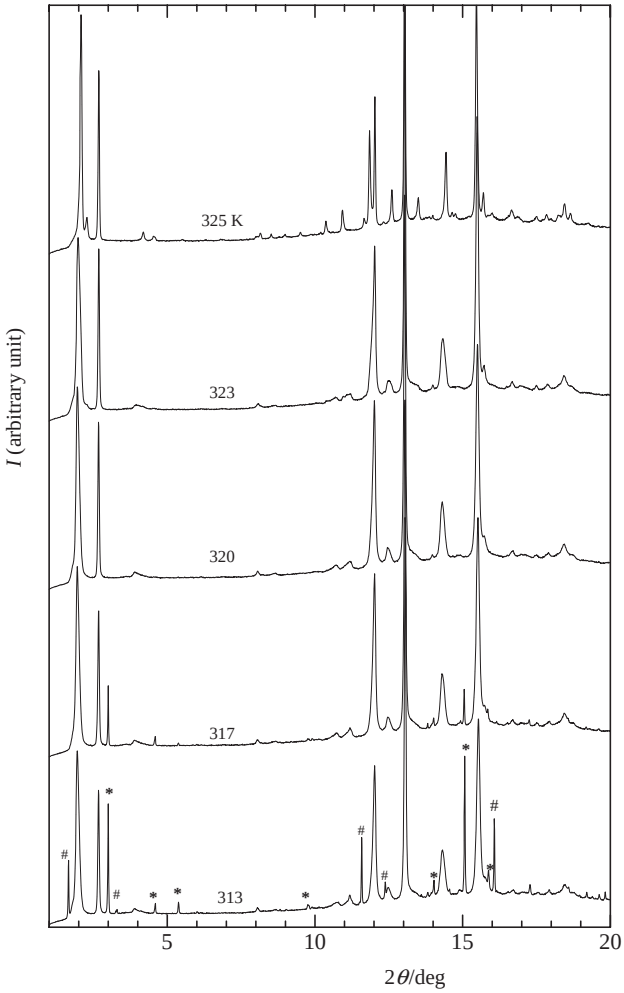

Fig. 4. Temperature dependence of XRD for **SP** of 7OCB. * and # denote peaks corresponding to **N** and **SP**, respectively.

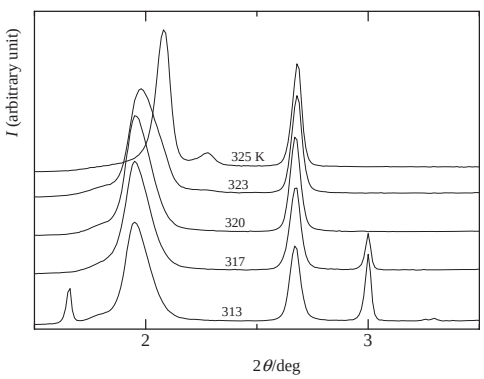

Fig. 5. Temperature dependence of XRD in the range of $2\theta = 1.5$–3.5° for **SP** of 7OCB.

intensity, while new peaks appear, several of which (designated by *) coincide with those of **N**. The peak at $2\theta = 15.1^\circ$ ($d = 3.82$ Å) is assigned as relatively strong ($1\bar{4}\bar{1}$) reflection of **N** by a simulation based on the single crystal structure with the program PULVERIX,[12] although only weak peaks are observed around 15° in the pattern of **N** in Fig. 3. The intensities of the peaks attributable to **N** decrease with the temperature rise and disappear at 320 K, the mp of **N**. On the other hand, new peaks, which do not coincide with those of **N** and are broader than those of **N**, behave differently. They remain almost constant and change slightly at 325 K. The peak at the lowest angle (1.95°) shifts to a slightly higher angle (2.08°), as shown in Fig. 5, and new peaks appear, resulting in essentially the same pattern as that of **CP**. Thus, the intermediate phase is a distinctly different crystalline phase from the most stable phase. The two structures may not be very different.

A sample obtained from **SP** kept at RT for 3 weeks gave broad peaks (designated by *), which coincide with those of the intermediate phase (not the most stable phase), as shown in Fig. 6.

It is concluded that **SP** stabilizes in two steps, first to the intermediate phase, which rearranges to the most stable phase at the melting point of the intermediate phase (324 K) or on keeping at RT for a longer time (several months).

Structural Features of the Most Stable Phases. Unit cell parameters of **CP** were determined in order to obtain information on the structures of the most stable phases by using the DASH program package. For 7OCB, a unique solution was obtained for a monoclinic cell based on 26 reflections: $a = 28.15$, $b = 7.438$, $c = 25.79$ Å, $\beta = 104.9^\circ$, $V = 5220$ Å^3, $Z = 12$, $d_X = 1.120$ g cm^{-3}. The indices are shown in Fig. 6. For 8OCB, slightly different 12 cells were obtained based on 18 reflections due to the several possibilities of assignments for higher-angle reflections: $a = 30.56$–30.62, $b = 7.39$–7.44, $c = 25.43$–25.52 Å, $\beta = 107.3$–107.8°, $V = 5481$–5520 Å^3, $Z = 12$, $d_X = 1.111$–1.118 g cm^{-3}. These results show that 7OCB and 8OCB have isomorphous structures with the com-

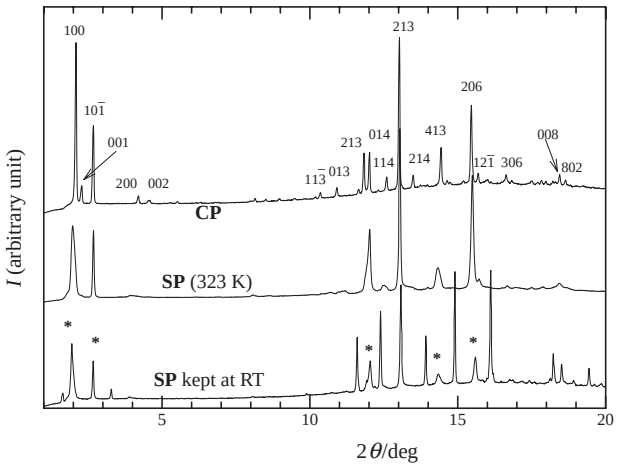

Fig. 6. Comparison of collapsed sample (kept at RT), intermediate phase, which appeared at 323 K on heating **SP**, and **CP**. * denotes newly observed peaks in the collapsed sample. For **CP**, *hkl*'s indexed by DASH[11] are shown.

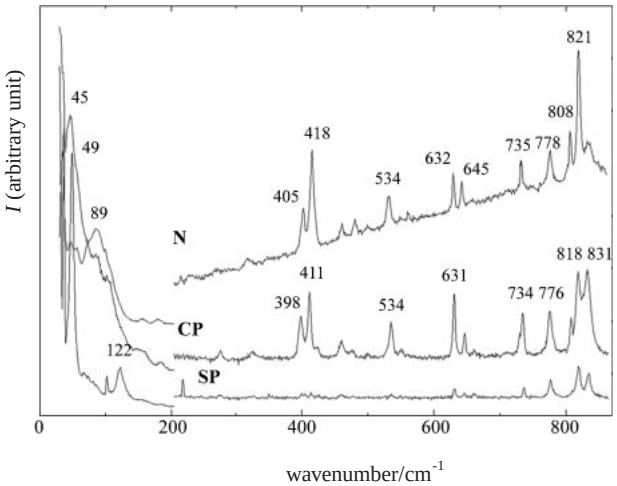

Fig. 7. Raman spectra of **N**, **CP**, and **SP** of 7OCB. Intensities are multiplied by 1/2 in lower frequency region (<200 cm^{-1}). Numerical numbers are wavenumbers.

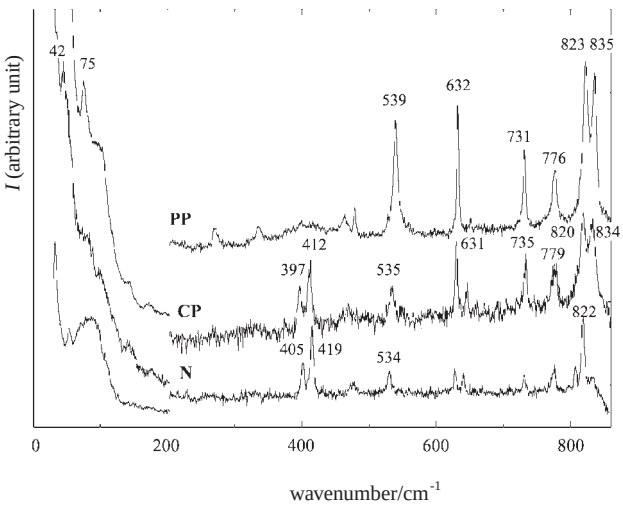

Fig. 8. Raman spectra of **PP**, **CP**, and **N** of 8OCB. Intensities are multiplied by 1/2 in lower frequency region (<200 cm^{-1}). Numerical numbers are wavenumbers.

mon *b* and *c* axes. The *a* axis is longer in 8OCB than in 7OCB, showing that the projection of each molecular long axis is along the *a* axis. The *a* axis are longer than the molecular lengths (the sums of distances between terminal atoms and van der Waals radii of the terminal N atom and methyl group), 22.8 and 24.1 Å for 7OCB and 8OCB, respectively. Thus, the structures have bimolecular layers stacked along the *a* axis. On the other hand, a relationship was found between the wavenumbers of CN stretching vibration band and the arrangements of CN groups in the crystalline states.[13] **CP** specimens of 7OCB and 8OCB showed the almost the same wavenumbers as 5OCB, in which one-dimensional chains of antiparallel arrangements of CN groups are formed.[14] Therefore, a similar CN–CN arrangement is also assumed for **CP** of 7OCB and 8OCB. Within the layers, molecular long axes are estimated to be tilted at 50° from the lengths of dimeric molecules in **N**, 42.9 and 45.4 Å for 7OCB and 8OCB, respectively. Unfortunately, however, the large *Z* value (12) shows that the structures are too complicated for us to determine the detailed structures from the powder data.

Raman Spectra of Crystalline Polymorphs at RT. Figures 7 and 8 show Raman spectra at RT of the different phases of 7OCB and 8OCB, respectively. The peak positions are summarized in Table 1 with the assignments for 8OCB and 9CB made by Merkel et al.[15] Bands at about 400 cm^{-1} are assigned to be the stretch vibrations of a twisted biphenyl link.[17] In the spectra of **SP** of 7OCB, it is interpreted that the band near here is almost negligible due to the orientation of the biphenyl link perpendicular to the wide plane of a single crystal,[9] to which the incident laser beam was perpendicular. On the other hand, the absence of any band in **PP** of 8OCB is caused by the planar biphenyl moiety.[18] The spectra of **N** of 7OCB and 8OCB are very similar, in accordance with the fact that their crystal structures are isomorphous.[18,19] The spectra of **CP** of 7OCB and 8OCB are also similar, confirming that they are isomorphous. The peaks around 400 cm^{-1} suggest that the biphenyl moieties are twisted in the most stable phases of 7OCB and 8OCB.

Spectral Change of 7OCB. The temperature dependence of the spectra was measured for the different polymorphs of 7OCB. The spectra of **CP** remained constant until its mp, 327 K. The spectra of **N** showed reduced peak intensities as a whole at 321 K and then the form changed to that of **CP** at 322 K. No significant change was observed up to 327 K: the most stable phase and the intermediate phase give the same Raman spectra. Figure 9 shows the temperature dependence of **SP**. At 303 K, bands around 400 cm^{-1} are almost absent. At 308 K, a band around 400 cm^{-1} begins to grow. At 313 K, the peaks at 401 and 412 cm^{-1} become clear, showing the appearance of the intermediate phase. However, the peak at 818 cm^{-1} is stronger than that at 833 cm^{-1} at 313 and 315 K. In the lower wavenumber region, the peak at 122 cm^{-1} becomes small and the broad peak at 79 cm^{-1} grows up. These facts suggest the coexistence of **N**. At 316 K and above, the intensities of the two peaks at 820 and 835 cm^{-1} become similar and the broad band at 79 cm^{-1} disappears, which are charac-

Table 1. Vibrational Wavenumbers (cm^{-1}) of Crystalline Polymorphs of 7OCB and 8OCB with the Assignments of 8OCB and 9CB Solids[15]

7OCB			8OCB			8OCB[15]		9CB[15]	
CP	**N**	**SP**	**CP**	**N**	**PP**				
45	51	49	42	56	75				
	58								
85	89			88	94				
100	160	122							
	183								
277 w	275 w				271.8 w				
324 w	322 w				334.5 w				
398.1 s	404.7 m		397.2 m	405.2 m					
411.0 s	418.2 s		411.6 s	418.5 vs					
460.4 w	461.5 w				464.0 w				
475 vw	482.6 w		469.1 w	480.8 w	478.8 w			~470	γCC
534.3 m	533.8 m		535.1 m	534.3 m	539.1 s	537.6	βCC(6a)		
				568.3 w		556.7	γCC(4)		
630.6 s	632.4 m	631.3 m	631.1 s	631.8 m	631.6 vs	633.8		637.3	βCC(6b)
645.8 w	645.3 m	644 vw	646.9 m	645.2 m	649.9 vw			648.9	δCCC+
		660 vw				661.4	δ_{def}COC		βCC(6b)
733.8 m	734.5 m	736 m	734.7 m	735.0 m	730.9 s	736.6	γCH	742.9	$\beta_{as}CH_2$+ γCH
776.1 m	778.0 m	776.8 s	778.7 m	779.2 m	776.4 m	780	βCC(1)	776.4	γCH(11)
806.6 m	808.5 m			811.4 m				811.9	νCCC+ βCC(1)+ $\beta_{as}CH_2$
818.4 vs	821.4 vs	817.9 vs	819.9 vs	822.0 vs	822.6 vs	821.4	γCH(10a)	823.9	
831.3 vs	837.3 w	833.1 s	833.9 vs	837.4 w	835.2 s	836.9	γCH(11)		

Wilson's symbols[16] for principal benzene bands are shown in parentheses.

teristic features for the intermediate or the most stable phases. Finally, melting begins at 327 K. In the melt (nematic phase), the peaks in 530–550 cm^{-1} become a broad band; a new peak at 785 cm^{-1} appears and the peaks in 800–830 cm^{-1} change their profile. All these changes are attributable to the melting of alkyl chains. From these results, we conclude that **N** coexists in the temperature range of 308–315 K. However, the spectral change was not reproducible. In many cases, simpler changes from **SP** to the intermediate phase were observed. This is considered to be due to the fact that two processes, transformation to **N** and direct stabilization, compete and **N** does not always appear in the very small area of samples.

In order to confirm this interpretation, we measured spectral changes, keeping the temperature constant (303 K). In one case, as shown in Fig. 10, the original spectrum of **SP** remained constant for the first 14 minutes, then a band near 400 cm^{-1} appeared and grew up into two peaks at 403 and 418 cm^{-1} after 21 minutes; the wavenumbers coincide with those of **N**. The peaks around 820 cm^{-1} also show the profile of **N**. In other cases, peaks appeared after a few minutes at 400–402 and 412–414 cm^{-1}, showing a direct stabilization to the intermediate phase to be dominant. From these results we conclude that the cross point of Gibbs energy lines of **SP** and **N** is below 303 K. In the DSC study, the endothermic peak shifted to the lower temperature with longer train on the low-temperature side, as the heating rate became slower, as was pointed out previously.[7] In the limit of infinitely slow heating, i.e. when the temperature is kept constant, the solid–solid phase transition temperature should be even lower.

In conclusion, two competitive processes, from **SP** to **N** and from **SP** to the intermediate phase, are confirmed. However, the **SP**–**N** transition is highly stochastic in the very small area of the samples, because the process includes nucleations of **N** in **SP**, while metastable **SP** tends to change directly to the more stable intermediate phase.

Spectral Change of 8OCB. The temperature dependence of the spectra was measured for the different polymorphs of 8OCB, except for **SP** which was too unstable to treat. The spectra of **CP** remained constant until its mp, 328 K. The spectrum of **N** changed to that of **CP** at 323 K, which changed again at 327 K. Figure 11 shows temperature dependence of **PP**. At 317 K, bands around 400 cm^{-1} have four peaks: at 397, 406, 413, and 420 cm^{-1}. The peaks at 397 and 413 cm^{-1} are attributable to those of **CP**, while those at 406 and 420 cm^{-1} to those of **N**, indicating that the two phases coexist. The dominant peak intensity at 820 cm^{-1} also supports the existence of **N**. At 324 K, only peaks at 399 and 414 cm^{-1} remain, showing the spectrum of **CP**. At the same time, the intensities of the two peaks in the 800 cm^{-1} region become equal. At 328 K, peaks at 460–480, 532–548, and 800–830 cm^{-1} become broad, due to the chain melting. From these results, it is confirmed that 8OCB has a phase transition from **PP** to **N**. However, in most cases, only peaks at 398 and 413 cm^{-1} appeared at 318 K, showing direct stabilization to **CP**. Then, we measured the spectral change while keeping the temperature at 317 K. In one case, as shown in Fig. 12, peaks around 400 cm^{-1} began to appear after 1 minute and grew up into the pattern of **N** with peaks at 404 and 418 cm^{-1}; the profile

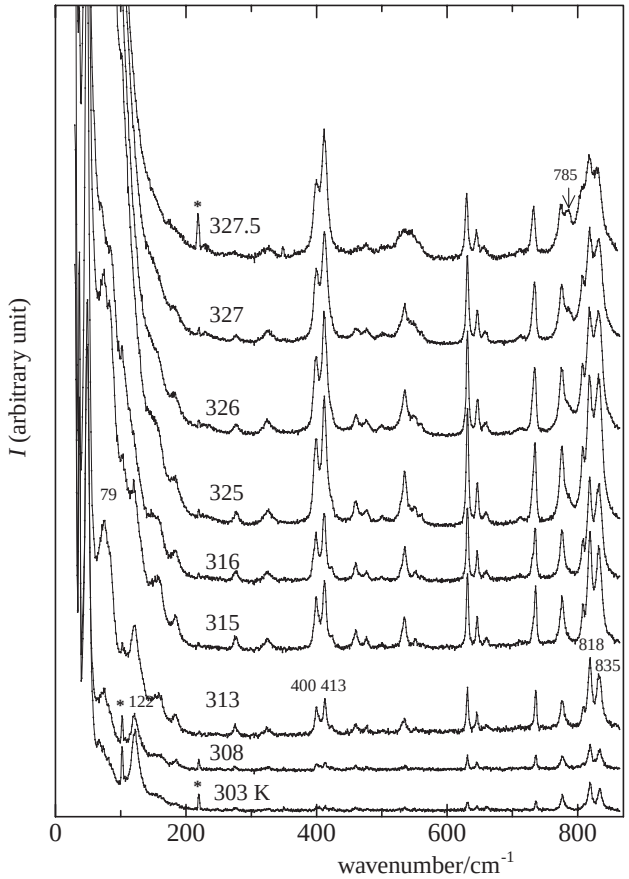

Fig. 9. Temperature dependence of Raman spectra for **SP** of 7OCB. * denotes plasma emission.

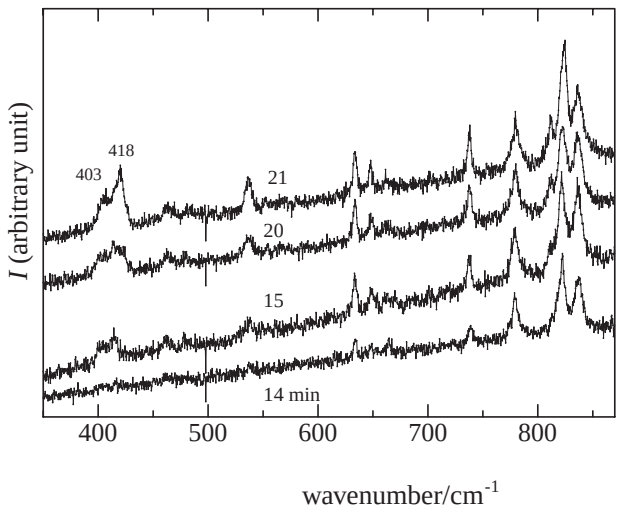

Fig. 10. Spectral change of **SP** of 7OCB obtained by keeping at 303 K.

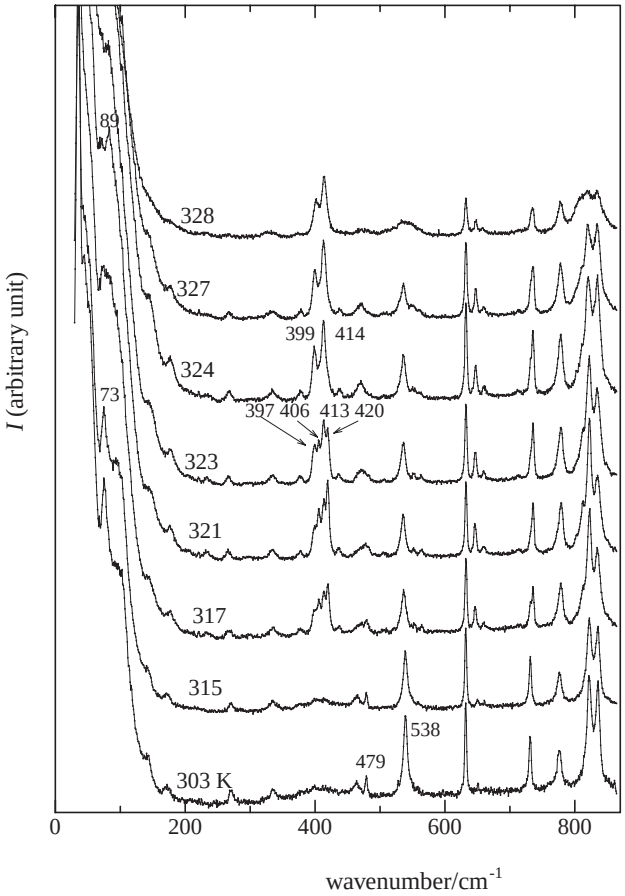

Fig. 11. Temperature dependence of Raman spectra for **PP** of 8OCB.

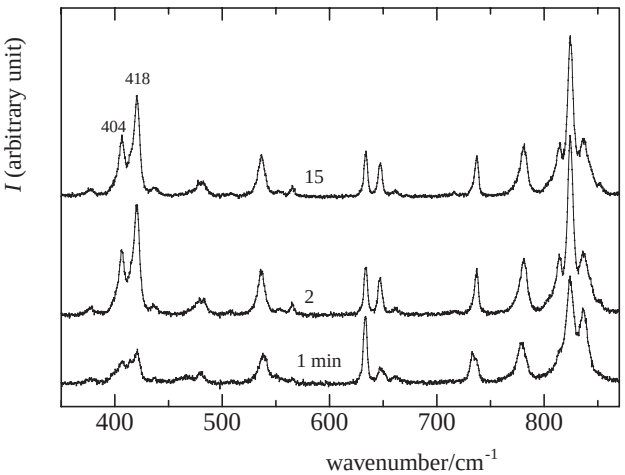

Fig. 12. Spectral change of **PP** of 8OCB obtained by keeping at 317 K.

around 820 cm^{-1} also corresponds to that of **N** after 2 minutes. The spectral features remained unchanged for longer than 15 minutes. In most cases, however, a slight change began to appear after 2 minutes and grew up into the pattern of **CP**. From these results, we conclude that two processes, from **SP** to **N** and from **SP** to **CP** are competitive and that once the nucleation of **N** occurs, **N** grows up immediately and retains at 317 K.

Conclusion

1. Temperature-dependent XRD studies and Raman spectral studies for 7OCB have confirmed the transition process between metastable phases **SP** to **N**, which were previously pro-

posed on the basis of the results of DSC, with structural evidence.

2. The XRD study shows that the intermediate phase of 7OCB appearing during the stabilization process is a slightly but definitely different crystalline phase from the most stable phase.

3. **SP** of 7OCB stabilizes in two steps, first to the intermediate phase, which rearranges to the most stable phase at the melting point of the intermediate phase (324 K) or on keeping at RT for several months or longer.

4. Unit cell parameters of the most stable phases of 7OCB and 8OCB have been derived from powder XRD, which, however, imply very complicated structures with $Z = 12$.

5. Temperature dependence of Raman spectra of 8OCB has confirmed the transition process between metastable phases **PP** to **N**, which were previously proposed on the basis of the results of DSC.

6. In the most stable phases of 7OCB and 8OCB, biphenyl links are twisted.

The synchrotron radiation experiments were performed at the BL02B2 in the SPring-8 with the approval of the Japan Synchrotron Radiation Research Institute (JASRI) (Proposal No. 2002A0403-ND1-np).

References

1 J. Bernstein, "Polymorphism in Molecular Crystals," Oxford Science Publications (2002).

2 E. V. Boldyreva, V. A. Drebushchak, I. E. Paukov, Y. A. Kovalevskaya, and T. N. Drebushchak, *J. Therm. Anal. Calorim.*, **77**, 607 (2004).

3 Q. Zhang, H. Chen, Y. Liu, and D. Huang, *Dyes Pigm.*, **63**, 11 (2004).

4 Recent examples: A. Tojima, H. Fujimaki, T. Manaka, and M. Iwamoto, *Thin Solid Films*, **438–439**, 440 (2003); A. Ghanadzadeh and M. S. Beevers, *J. Mol. Liq.*, **102**, 365 (2003).

5 S. C. Jain, S. A. Agnihotry, and V. G. Bhide, *Mol. Cryst. Liq. Cryst.*, **88**, 281 (1982).

6 S. C. Jain, S. A. Agnihotry, S. Chandra, and V. G. Bhide, *Mol. Cryst. Liq. Cryst.*, **104**, 161 (1984).

7 K. Hori, Y. Koma, M. Kurosaki, K. Itoh, H. Uekusa, Y. Takenaka, and Y. Ohashi., *Bull. Chem. Soc. Jpn.*, **69**, 891 (1996).

8 K. Hori and H. Wu, *Liq. Cryst.*, **26**, 37 (1999).

9 J. Tanno, K. Itoh, A. Tsuji, and K. Hori, *J. Mol. Struct.*, **379**, 121 (1996).

10 E. Nishibori, M. Takata, K. Kato, M. Sakata, Y. Kubota, S. Aoyagi, Y. Kuroiwa, M. Yamakata, and N. Ikeda, *Nucl. Instrum. Methods Phys. Res., Sect. A*, **467–468**, 1045 (2001).

11 I. F. David, K. Shankland, and N. Shankland, *Chem. Commun.*, **1998**, 931; For indexing: A. Boultif and D. Louer, *J. Appl. Crystallogr.*, **24**, 987 (1991).

12 "PULVERIX," K. Yvon, W. Jeitschko, and E. Parthe, University of Geneva.

13 K. Hori, M. Kuribayashi, and M. Iimuro, *Phys. Chem. Chem. Phys.*, **2**, 2863 (2000).

14 P. Mandal and S. Paul, *Mol. Cryst. Liq. Cryst.*, **131**, 223 (1985).

15 K. Merkel, R. Wrzalik, and A. Kocot, *J. Mol. Struct.*, **563–564**, 477 (1996).

16 H. W. Wilson and J. E. Bloor, *Spectrochim. Acta*, **21**, 45 (1965).

17 A. Takase, S. Sakagami, and M. Nakamizo, *Jpn. J. Appl. Phys.*, **17**, 1495 (1978).

18 K. Hori, M. Kurosaki, H. Wu, and K. Itoh, *Acta Crystallogr.*, **C52**, 1751 (1996).

19 K. Hori, Y. Koma, A. Uchida, and Y. Ohashi, *Mol. Cryst. Liq. Cryst.*, **225**, 15 (1993).